NRL Report 8391

Plastic Deformation and Ductile Fracture at an Angled Slit in a Sheet Under Tension

S. C. SANDAY

Composite Materials Branch
Material Science and Technology Division

AND

O. RICHMOND

U.S. Steel Research Laboratory
Monroeville, PA 15146

March 17, 1980

NAVAL RESEARCH LABORATORY
Washington, D.C.

Approved for public release; distribution unlimited.

SECURITY CLASSIFICATION OF THIS PAGE (When Data Entered)

REPORT DOCUMENTATION PAGE		READ INSTRUCTIONS BEFORE COMPLETING FORM
1. REPORT NUMBER NRL Report 8391	2. GOVT ACCESSION NO.	3. RECIPIENT'S CATALOG NUMBER
4. TITLE (and Subtitle) PLASTIC DEFORMATION AND DUCTILE FRACTURE AT AN ANGLED SLIT IN A SHEET UNDER TENSION		5. TYPE OF REPORT & PERIOD COVERED Final report (period covering 1977-1979) 6. PERFORMING ORG. REPORT NUMBER
7. AUTHOR(s) S. C. Sanday and O. Richmond*		8. CONTRACT OR GRANT NUMBER(s)
9. PERFORMING ORGANIZATION NAME AND ADDRESS Naval Research Laboratory Washington, DC 20375		10. PROGRAM ELEMENT, PROJECT, TASK AREA & WORK UNIT NUMBERS 61153N RR0220441 NRL Problem 63-1047-0-0
11. CONTROLLING OFFICE NAME AND ADDRESS Department of the Navy Office of Naval Research Arlington, VA 22217		12. REPORT DATE March 17, 1980 13. NUMBER OF PAGES 19
14. MONITORING AGENCY NAME & ADDRESS(if different from Controlling Office)		15. SECURITY CLASS. (of this report) UNCLASSIFIED 15a. DECLASSIFICATION/DOWNGRADING SCHEDULE

16. DISTRIBUTION STATEMENT (of this Report)

Approved for public release; distribution unlimited.

17. DISTRIBUTION STATEMENT (of the abstract entered in Block 20, if different from Report)

18. SUPPLEMENTARY NOTES

*U.S. Steel Research Laboratory, Monroeville, PA 15146

19. KEY WORDS (Continue on reverse side if necessary and identify by block number)

Fracture mechanics	Metal sheet	Hard-rolled copper
Stress analysis	Plastic zone length	Moiré grids
Complex stress state	Plastic zone direction	Oblique lighting photography
Elastic-plastic deformations	Necking	
Oriented slit	Failure criterion	

20. ABSTRACT (Continue on reverse side if necessary and identify by block number)

A theoretical solution is obtained for the growth of narrow plastic zones and for the initiation of ductile fracture at the ends of an angled slit in a metal sheet under remote uniform tension. The theoretical model assumes two distinct regions: narrow plastic zones at the ends of the slit caused by necking of the sheet, and a surrounding elastic region. The direction of the narrow plastic zones is assumed to be normal to the remote tension regardless of the slit angle. The length of the plastic zones is assumed to be governed by Dugdale's hypotheses of yield stress attainment along the plastic

(Continues)

DD FORM 1 JAN 73 1473 EDITION OF 1 NOV 65 IS OBSOLETE
S/N 0102-014-6601

SECURITY CLASSIFICATION OF THIS PAGE (When Data Entered)

20. Abstract (Continued)

zone-elastic region boundary and continuity of stress at the end of the plastic zone. Finally, fracture initiation is postulated to occur at the ends of the slit when the ratio of slit opening displacement to plate thickness attains a critical value representative of the material ductility. Experimental results on hard-rolled copper sheets support the assumptions and closely match the predicted results.

CONTENTS

INTRODUCTION 1

THEORETICAL MODEL 2

Neck Direction 3
Plastic Zone Length 4
Fracture Initiation 8

EXPERIMENTAL RESULTS 8

DISCUSSION 10

CONCLUDING REMARKS 14

REFERENCES 15

NOMENCLATURE 16

PLASTIC DEFORMATION AND DUCTILE FRACTURE AT AN ANGLED SLIT IN A SHEET UNDER TENSION

INTRODUCTION

Experimental observations on the failure of uniaxially stretched metal sheets with central slits may, on the basis of sheet thickness, be classified into three types as shown in Fig. 1. For very thin sheets (foils) buckling is observed around the slit, with large out-of-plane elastic deflections; for thicker sheets plastic thinning, or necking, occurs at the ends of the slit; and, for still thicker sheets (plates) heart-shaped plastic zones occur at the ends of the slit with very little thinning.

The present work is restricted to the necking type failure and includes both a theoretical model and its experimental verification. It is clear from the outset that neither a plane stress nor a plane strain model is adequate because of the extensive thinning in the plastic zones. Dugdale [1], however, assumed that the plastic zones could be treated as narrow extensions of the slit with normal traction at the elastic-plastic boundary equal to the yield stress Y, and stress continuity at the ends. He thus reduced the solution in the elastic region to one of plane stress. For the case where the slit is normal to the applied stress, he determined a relationship between the plastic zone length s, and the uniform applied stress T:

$$\frac{s}{a} = \sec\left(\frac{\pi}{2}\frac{T}{Y}\right) - 1, \tag{1}$$

where $2a$ is the original slit length. Using the same model, Goodier and Field [2] and Burdekin and Stone [3] determined a relationship between the opening displacement u_e, at the ends of the slit and the plastic zone length:

$$\frac{u_e}{a} = \frac{8Y}{\pi E}\ln\left(1 + \frac{s}{a}\right), \tag{2}$$

where E is Young's modulus. Arguing that fracture is controlled by in-plane strains, they proposed that slit propagation would occur when s/a reached a critical value. Hahn and Rosenfield [4], however, recognizing the out-of-plane nature of the plastic deformation, proposed that crack propagation would occur when the longitudinal strain ϵ_ℓ at the ends of the slit equalled that at fracture in a standard tensile specimen. They assumed plane strain in the neck with zero strain in the neck direction, and estimated the strain to be given by

$$\epsilon_\ell = \frac{2u_e}{t_i}, \tag{3}$$

Manuscript submitted January 4, 1980.

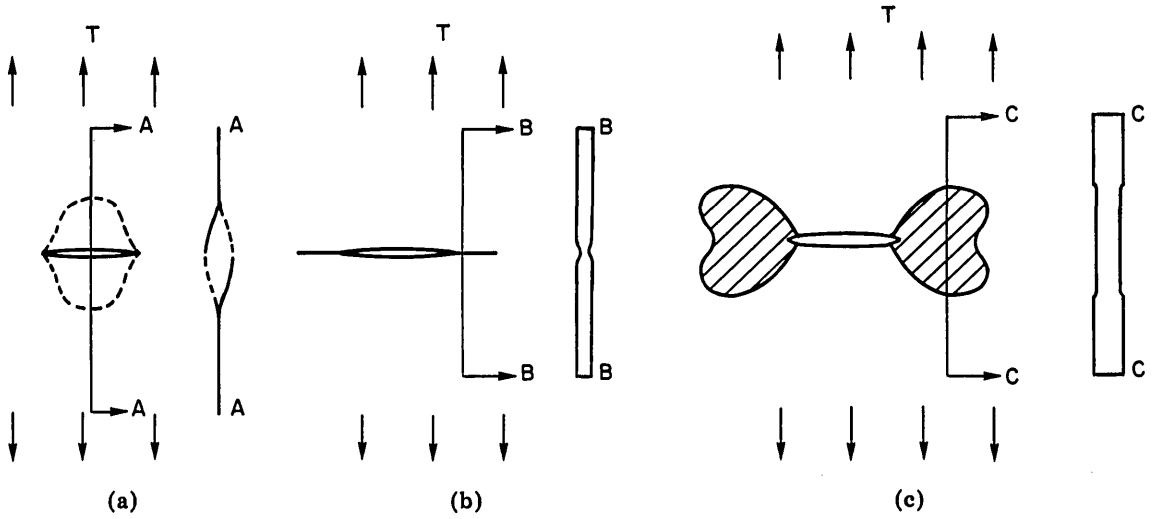

Fig. 1—Effect of plate thickness on mode of deformation in plates with central slits: (a) buckling mode in a foil; (b) necking mode in a sheet; and (c) plane strain mode in a plate

where t_i is the initial sheet thickness. Isherwood and Williams [5], employing a similar model, proposed that fracture would occur when the through-thickness strain ϵ_t at the ends of the slit equalled that at fracture in a standard specimen. Using the plane strain theory of necking due to Lee [6] and Onat and Prager [7], they computed this value to be

$$\epsilon_t = -\frac{t_i - t}{t_i} = -\frac{u_e}{t_i}, \tag{4}$$

where t is the current value of sheet thickness at the ends of the slit.

All of the aforementioned work has been restricted to the case of a slit normal to the applied load. In recent years, however, a number of studies have been undertaken on angled slits motivated by a desire to understand fracture in mixed-mode deformation or in complex stress states. All of these have been restricted to brittle fracture whereas the present study is aimed specifically at extending the Dugdale model of ductile fracture, as interpreted by Hahn and Rosenfield, to the angled slit situation. A complete theoretical model is presented here together with experimental verification. Because Clausing [8] has shown that there is no unique relationship between the values of critical fracture strain in plane strain and in simple tension, it is suggested that the critical fracture strain at the tip of the slit must be determined from a plane strain tensile test.

THEORETICAL MODEL

An infinite sheet of thickness t_i is assumed to be uniaxially stretched at infinity by a uniform traction T. The sheet has a thin central slit of length $2a$ at an angle $\gamma\pi$ to the normal of the applied traction as shown in Fig. 2. Monotonic increase of the traction results in plastic zones of length s and width u growing from each end of the slit at an angle $\Omega\pi$.

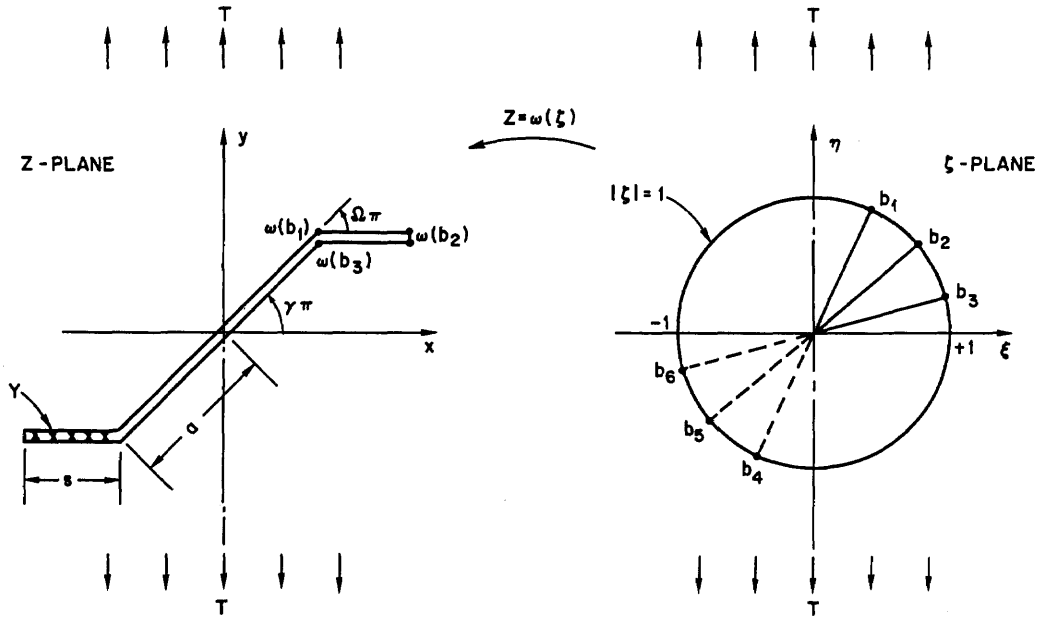

Fig. 2 — Conformal mapping of idealized slit and plastic zone geometry (for $\Omega = \gamma$) onto the unit circle

The out-of-plane deformation within these zones leads to localized necking. After a critical amount of thinning of the sheet takes place, extension of the slit (fracture) begins. The first concern is to justify the assumed direction of the plastic zones at the ends of the slit. The second goal is to determine relationships between the applied traction, the length of the plastic zones, and the slit opening displacements for various slit angles. Finally, a relationship is sought between the opening displacement and the thinning (necking) of the sheet within the plastic zone such that, at a critical value of through-thickness strain at the ends of the slit, fracture initiation may be predicted.

Neck Direction

It is assumed that the plastic zone will grow in the plane of the sheet in the direction normal to the principal tensile stress direction, i.e., $\Omega = \gamma$. This assumption is fully supported by the experimental evidence to be presented below. It is also consistent with a theoretical argument based on analytical solutions. Griffith [9] and later McClintock [10], taking the slit to be the limit of an elliptical hole as the minor axis vanishes, showed that at the end of the slit, this angle is given by

$$\Omega = \gamma/2. \tag{5}$$

On the other hand, Erdogan and Sih [11] used William's solution [12] for a slit to show that the angle is given by

$$\frac{\sin \Omega\pi}{1 - 3 \cos \Omega\pi} = \tan \gamma\pi. \tag{6}$$

In studying this paradox, Cotterell [13] observed that a crack at an elliptical hole in a brittle material, polymethylmethacrylate, started in the direction predicted by Eq. (5) but turned very quickly to a direction more like that given by Eq. (6). Williams and Ewing [14], however, demonstrated that even Eq. (6) does not properly predict the direction of fracture propagation when the slit direction approaches that of the applied traction. They also showed, although their solution contained a small error as pointed out by Finnie and Saith [15], that much better agreement with experiments is obtained if the principal stress direction is taken at a small distance from the slit tip. It should be noted that this artifice gives a solution which tends toward the normal to the remote tension as the distance from the tip increases, i.e., toward

$$\Omega = \gamma. \tag{7}$$

Marinshaw and Lindsey [16] obtained results on propellant materials which also agree more closely with Eq. (7) than with Eq. (6). For these reasons as well as the fact that necking involves a greater portion of the material next to the slit than does brittle fracture, Eq. (7) is assumed here to give the direction of plastic zone growth.

Plastic Zone Length

The elastic solution for the plane stress region outside of the slit and plastic zones is an extension of the Dugdale solution for a normal slit to the case of arbitrarily oriented slits. The complete solution is quite lengthy and is presented in detail elsewhere [17]. Only an outline of the procedures is given here. Muskhelishvili's method [18] was used, and efficient use of this method requires determining first the analytic function that conformally maps the region outside of the polygonal shape representing the slit and plastic zones onto the outside of a unit circle as illustrated in Fig. 2. This function, which is a special case of the Schwarz-Christoffel formula, is given by [19]

$$z = \omega(\zeta) = \int^{\zeta} \left(\frac{\zeta^2 - b_1^2}{\zeta^2 - b_3^2} \right)^{\gamma} \left(1 - \frac{b_2^2}{\zeta^2} \right) d\zeta, \tag{8}$$

where $b_j = e^{i\beta_j}, j = 1, 2, 3$ defines the points on the unit circle corresponding to the vertices of the polygon. Only three vertices appear since the others have been included by symmetry. A choice of β_1 and β_2 determines the lengths of the slit and the plastic zones. Then β_3 must be taken such that the length in the z-plane between the vertices 1 and 2 is the same as that between the vertices 2 and 3.

Expansion of Eq. (8) results in an infinite series which must be truncated and evaluated on the unit circle. Because this procedure leads to multivalence, the truncated series is evaluated on a circle $1 + \delta$, where $\delta \ll 1$. The magnitude of δ is chosen to preserve univalence, and it is inversely proportional to the number of terms retained in the series. The desired mapping function is

$$\omega(\zeta) = B(\zeta + a_1\zeta^{-1} + a_2\zeta^{-2} + \cdots + a_n\zeta^{-n}), \tag{9}$$

where the a's are complex-valued coefficients and B is a magnification and rotation constant.

The solution is then obtained by finding the proper boundary function $F(\sigma)$ to introduce into the boundary condition

$$\phi(\sigma) + \frac{\omega(\sigma)}{\overline{\omega'(\sigma)}}\,\overline{\phi'(\sigma)} + \psi(\sigma) = F(\sigma), \tag{10}$$

where $\phi(\sigma)$ and $\psi(\sigma)$ are the values of the stress functions

$$\phi(\zeta) = \sum_{k=1}^{n} c_k\,\zeta^k \text{ and } \psi(\zeta) = \sum_{k=1}^{n} d_k\,\zeta^k$$

(which must satisfy the biharmonic equation) at the boundary $\zeta = \sigma = e^{i\upsilon}$.

Thus, when the functions ω, F, ϕ, and ψ are introduced into Eq. (10), equating coefficients of like power terms leads to a set of simultaneous algebraic equations in the unknown c's and d's which, when found, determine the desired stress functions. Then the stresses and displacements can be obtained through the standard formulae [18]:

$$\sigma_{\rho\rho} + \sigma_{\upsilon\upsilon} = 4Re\,\Phi(\zeta) = 2\left[\Phi(\zeta) + \overline{\Phi(\zeta)}\right], \tag{11}$$

$$\sigma_{\upsilon\upsilon} - \sigma_{\rho\rho} + 2i\sigma_{\rho\upsilon} = \frac{2\zeta^2}{\rho^2\,\overline{\omega'(\zeta)}}\left\{\overline{\omega(\zeta)}\;\Phi'(\zeta) + \omega'(\zeta)\,\Psi(\zeta)\right\}, \tag{12}$$

and

$$2\mu\,|\omega'(\zeta)|\,(v_\rho + iv_\upsilon) = \frac{\overline{\zeta}}{\rho}\,\overline{\omega'(\zeta)}\quad\left\{\kappa\phi(\zeta) - \frac{\omega(\zeta)}{\overline{\omega'(\zeta)}}\,\overline{\phi'(\zeta)} - \overline{\psi(\zeta)}\right\}, \tag{13}$$

where

$$\Phi(\zeta) = \frac{\psi_1'(\zeta)}{\omega'(\zeta)},$$

$$\Psi(\zeta) = \frac{\psi'(\zeta)}{\omega'(\zeta)},$$

$$\mu = \frac{E}{2(1+\nu)},$$

and

$$\kappa = \frac{3-\nu}{1+\nu}.$$

The boundary conditions must be such that the stresses are specified either at infinity or at finite points of the boundary but not at both simultaneously. Moreover, the constant uniform boundary stresses at finite points should be either normal or tangent to the boundary. The given problem is thus decomposed into four component problems A through D satisfying these requirements: Problem A) a uniform tensile stress of magnitude $(T - Y)$ is applied normal to the plastic zone boundary; Problem B) a uniform tensile stress of magnitude $T \cos^2 \gamma\pi$ is applied normal to the slit boundary; Problem C) a uniform shear stress of magnitude $T \sin \gamma\pi \cos \gamma\pi$ is applied over the slit boundary; and Problem D) a uniform tensile stress of magnitude T is applied at infinity (say in the y-direction). Each of these component problems is then solved in the ζ-plane and the results transformed to the physical z-plane, where linear superposition is invoked to yield the final solution [17]. The nature of the mapping function, Eq. (8), necessitates the use of an efficient code in a large memory, fast digital computer to obtain accurate results.

The elastic solution, as expected, possesses a stress singularity at the tip of the plastic zone. This singularity may be eliminated by imposing an appropriate continuity condition. Following Dugdale [1], the plastic zone length should be such that the maximum principal stress in the elastic region just outside the plastic zone tip equals the assumed yield stress just inside it.

This condition could be invoked and the length s adjusted until the two stresses are nearly equal for a fixed value of the applied stress T. However, this lengthy iterative procedure is unnecessary since, in order to obtain the desired information over the whole range of plastic zone length s, the following converse procedure may be used: the elastic stress just outside the plastic zone tip has the value Y for some chosen value of s provided the correct value of T can be found. This value of T is found from the condition

$$\sigma^*_A (T - Y) + T\sigma^*_B + T\sigma^*_C + T = Y, \tag{14}$$

where σ^*_J ($J = A, B, C$) are the tangential stresses just outside the tip of the plastic zone due to unit applied tractions at the slit-plastic zone boundary (as calculated from Eqs. (11) and (12)), and the term T arises from the corresponding stress due to the applied traction at infinity.

Thus, from Eq. (14) the dimensionless ratio T/Y is calculated as a function of the dimensionless ratio s/ℓ, where $\ell = a + s$, with the orientation of the slit given by the parameter γ. These results, for several values of γ, are shown in Fig. 3.

To further justify the correctness of the assumed direction for the plastic zone the yield condition (i.e., $0 \leqslant \sigma_{\theta\theta} \leqslant Y$) was systematically verified just outside the boundary of the plastic zone.

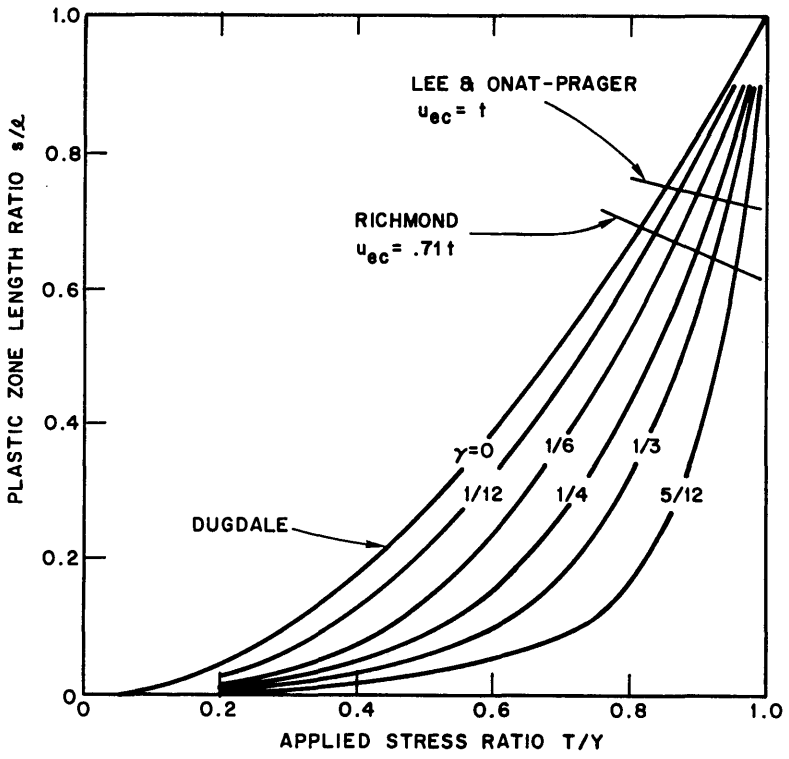

Fig. 3 — Calculated length of plastic zone vs applied stress as a function of slit angle showing upper limit for initiation of slit extension according to different plastic solutions

Fracture Initiation

As it was assumed above, plastic deformations occur in the direction normal to the sheet (necking) and propagate in the direction normal to the applied traction at infinity. This leads to a condition of plane strain where the deformation along the direction of plastic zone growth is constrained by the adjacent elastic region. Thus, a small element at the tip of the slit may be viewed as a bar under uniaxial traction and in a state of plane strain, whose solution, for the case of a rigid-perfectly plastic material behavior, is a special case of the solution for notched bars with notch angle equal to π. Solutions for this problem are due to Lee [6] and Onat and Prager [7] for a quasi-steady case, and to Richmond [20] for a nonsteady case. They relate the displacement between two points on either side of the plastically deformed region (or equivalently the minimum thickness of the neck) to the original thickness of the bar.

It is suggested here that growth initiation takes place when the displacement u_e between two points on either side of the plastically deformed neck just at the tip of the slit, as calculated from the elastic solution, attains a critical value. This critical value is a function of the thickness of the sheet t_i, in accordance with Richmond's solution, and of the ductility of the material. In general, one test is necessary to determine the plane strain ductility of the material. However, when the ductility is such that the neck may develop fully and separation takes place at a sharp edge such a test is unnecessary since the solution provides the critical value as well. For this case, the Lee and Onat-Prager solutions predict the critical displacement u_{ec} to be 1.0 t_i while the Richmond solution predicts a value of 0.71 t_i.

Therefore, since the displacement u_e is uniquely related to the plastic zone length s for each slit orientation γ, the theoretical results using the suggested criterion for the case of a fully developed neck constitute an upper bound for slit growth initiation. The various plastic solutions have different upper bounds as shown in Fig. 3.

EXPERIMENTAL RESULTS

The experiments were performed to assess the predictive capabilities of the theoretical model and, consequently, needed to be only few in number and limited in scope. However, careful experimental control from the first step of material selection to the final step of measuring the pertinent parameters had to be maintained.

The criterion used for material selection was the closeness of agreement between the material response to uniaxial tensile traction and the elastic-perfectly plastic constitutive relation assumed in the model. Hard rolled 99.9% pure copper sheet 0.0036 in. thick was selected. Tensile load-displacement relationships were determined using specimens of the type shown in Fig. 4, but without the slit. Loads were recorded on a 10,000 lb capacity Instron universal testing machine with a 1,000 lb capacity load cell; displacements were obtained from Moiré grid interference patterns. The material response to uniaxial tension is shown graphically in Fig. 5.

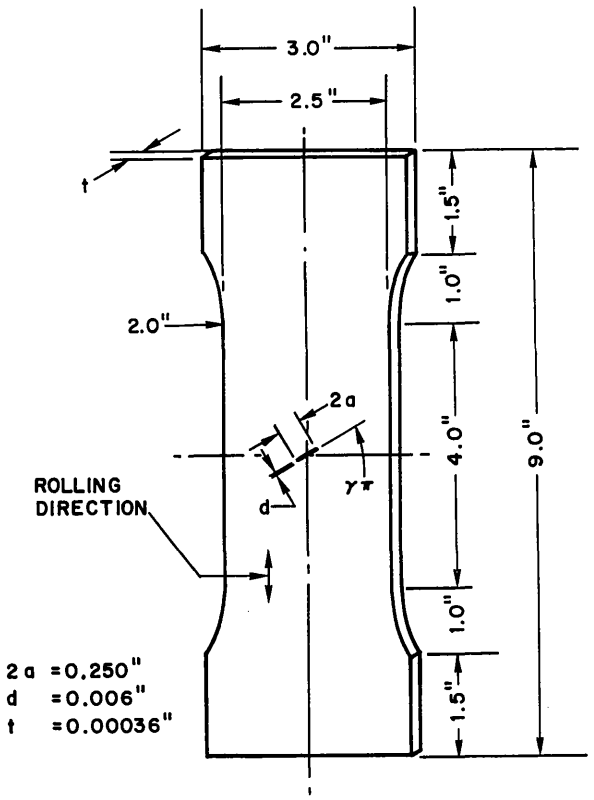

Fig. 4 — Sheet specimen geometry

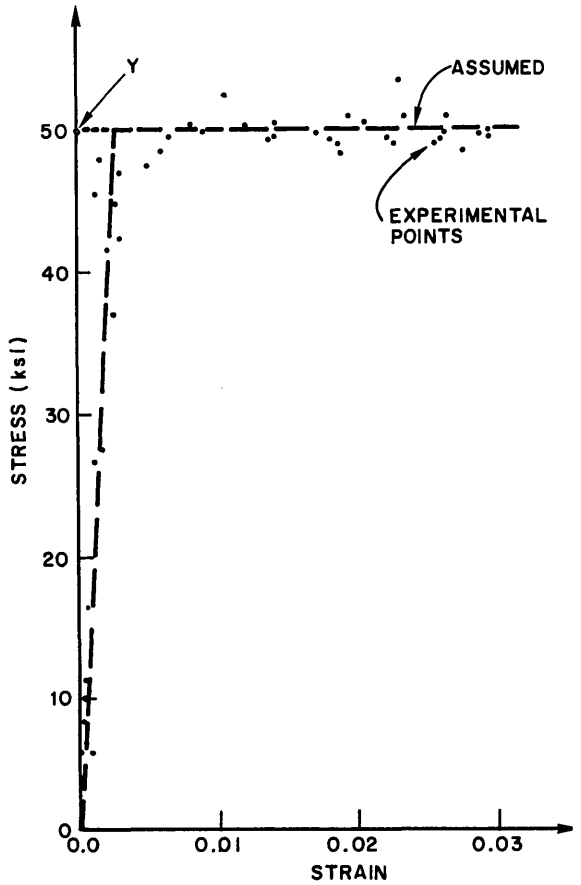

Fig. 5 — Uniaxial stress-strain relationship for hard-rolled copper sheet

The specimen geometry shown in Fig. 4 was chosen by establishing reasonable upper and lower bounds for dimensions and ratios of dimensions that would occur both prior to and during the tests. The pertinent factors were testing facilities, measuring techniques, machining capabilities, isotropy of the test material, prevention of buckling, approximation of boundary conditions, system rigidity, and the need for a large stress concentration.

The ends of the slit are semicircular, with a root radius equal to half the width of the slit, so that, regardless of slit orientation γ, the stress concentration would remain as nearly constant as possible.

The angle between the slit and the perpendicular to the applied traction, given by $\gamma\pi$, was arbitrarily chosen to vary from 0° to 75° in steps of 15° (i.e., γ = 0, 1/12, 1/6, 1/4, 1/3, 5/12).

The tests were conducted at room temperature (20°C) using quasi-static displacement rates (~0.8 μm/s). Load and cross-head displacement were monitored continuously during the tests using a conventional *X-Y* recorder. However, measurement of the strain distribution in the gage length of the specimen required special care. Optical interference grids were constructed by printing a 310/inch grid directly on the front surface of the specimen and covering this with a glass plate upon which a reference grid of 300 lines/inch had been printed. As the specimen deformed under load, an interference pattern was produced which was then photographed periodically.

The development of the plastic enclaves was also recorded photographically using oblique lighting through a glass plate on the back surface of the specimen. Figure 6 typifies this record for each value of γ. Sandwiching the specimen between the reference grid glass plate and the spring loaded backup glass plate served also to minimize buckling of the specimen with negligible effect on the recorded load.

The experimental results are summarized in Fig. 7, where the data points are superposed on reproductions of the curves of Fig. 3. Each point is the average of the values measured in five duplicate experiments. Concerning experimental accuracy, it is estimated that the load was measured to within 5% and the plastic zone geometry to within 7% of the exact values. Also shown in Fig. 7 is the locus of points where extension of the slit initiates.

The postfracture profile of the neck within the plastic region was determined by mounting and sectioning the nickel plated (after testing) specimen and photographing the sections. Figure 8 shows a typical section in which the theoretical profiles predicted by the Lee and Onat-Prager solutions and by the Richmond solution have been included.

DISCUSSION

The experimental data gathered to test the assumptions made in the formulation of the theoretical model fall into three categories: material behavior, initial and developed geometry, and loading boundary condition. Excellent agreement between the assumed and actual material responses to uniaxial tension is shown graphically in Fig. 5. Larger plastic deformations would have been preferable, but these could be obtained in commercially available materials only at the expense of reduced thickness uniformity and reduced percentage of cold reduction. The latter condition invariably results in a lower elastic modulus and a longer nonlinear stage before attaining maximum load. Approximating an infinite sheet by a suitable finite specimen geometry was judged satisfactory because the Moiré patterns were quite uniform toward the edges as well as at the upper and lower ends of the gage section. The most significant features of the assumed developed geometry under loading were justified beyond doubt. Oblique lighting photographs showed that initiation of plastic flow takes place in the semicircular tip of the slit at the point where the applied traction is tangent to it and that the plastic zone grows in a thin band along a path perpendicular to it (within 2°). Moreover, the out-of-plane deformations lead to the formation of a convex neck. An example of these observations is shown in Figs. 6 and 8. Finally, the assumed uniformity of the applied traction was evaluated also by the transverse uniformity of the Moiré patterns at either end of the specimen's gage section.

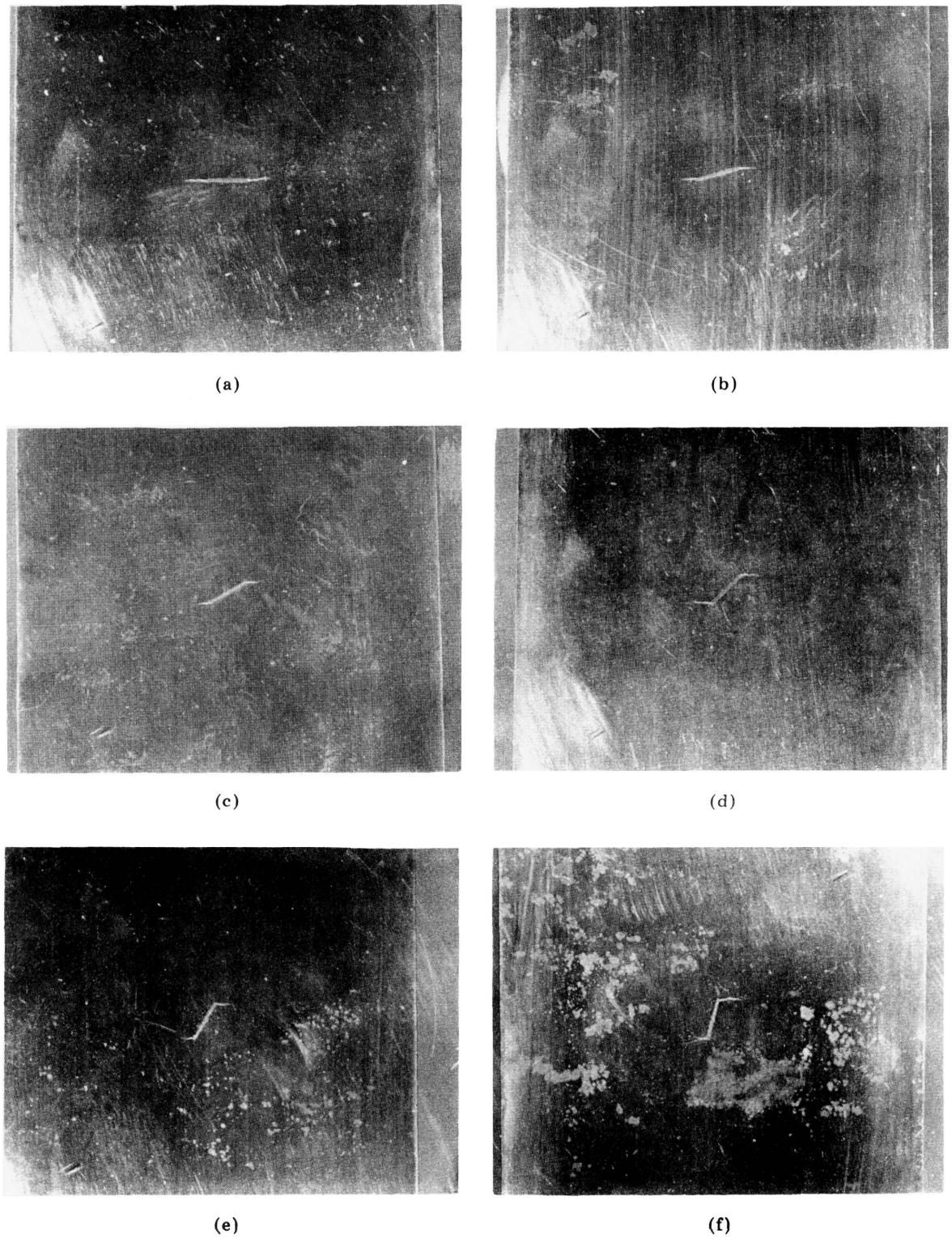

Fig. 6 — Oblique lighting photographs of copper sheet specimens with slits ($\gamma\pi$ = 0, 15, 30, 45, 60, 75°) showing the plastic zones caused by uniaxial tensile stress applied in the vertical direction

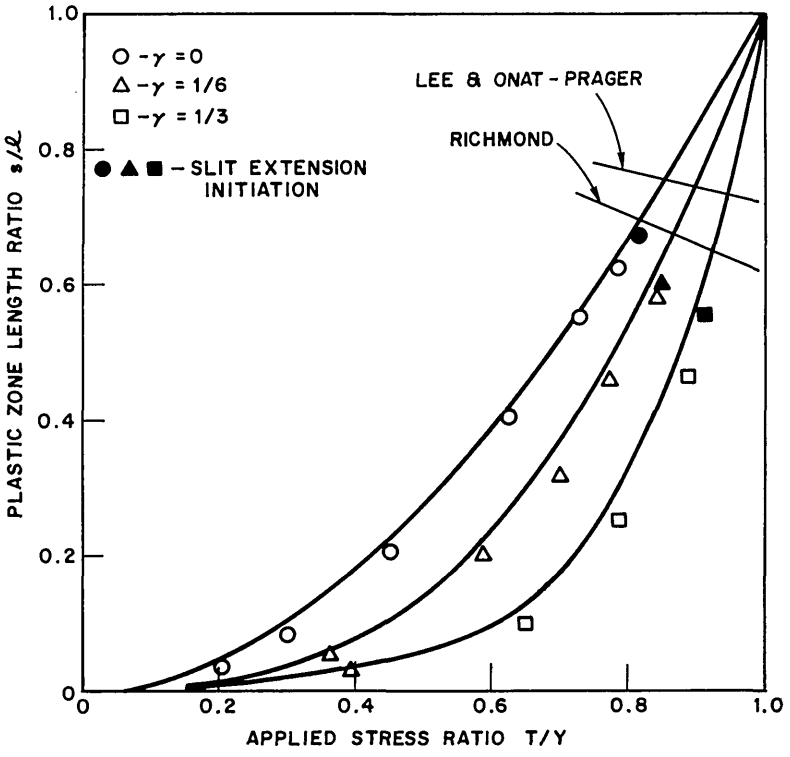

Fig. 7 — Experimental length of plastic zone up to initiation of slit extension as a function of slit angle and applied stress

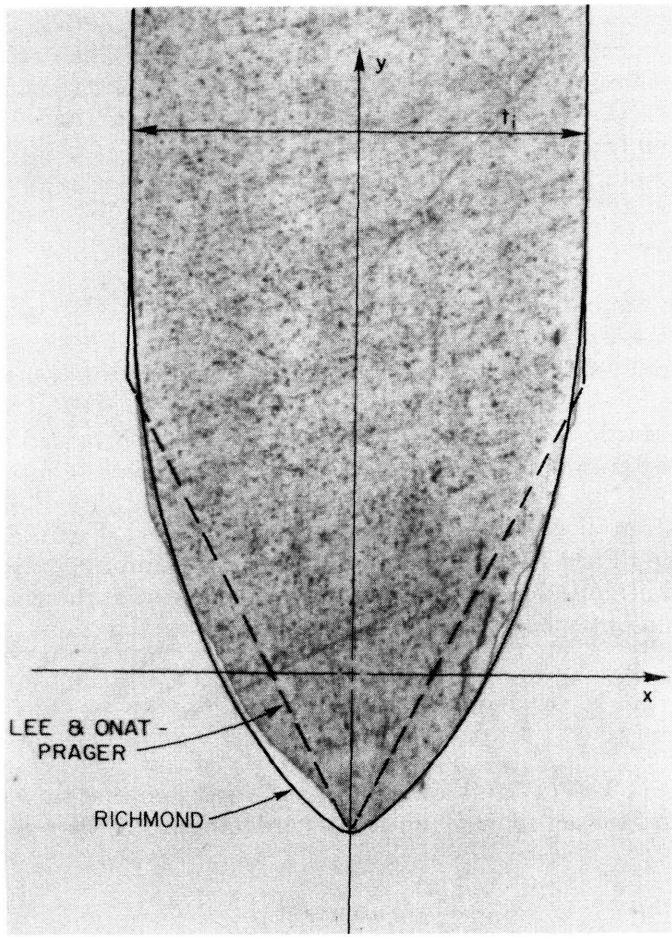

Fig. 8 — Experimental and theoretical neck geometries

In general, the relationship between the applied traction, the plastic zone length, and the slit orientation found experimentally agrees well with the relationship predicted by the theoretical model. In fact, the differences fall within the experimental error up to a T/Y ratio of about 0.7. The discrepancy for T/Y ratios between 0.7 and the upper limit for slit growth initiation may be explained by considering the following four factors: (a) The ratio of average net section stress to yield strength of the material, T_{net}/Y, should not exceed the approximate value of 0.8 for reasons detailed elsewhere [21-23]. When this ratio approaches 0.8, the plastic zone length should be expected to *increase* rapidly. This was indeed observed here. (b) The second factor is buckling of the sheet in the vicinity of the slit, which would lead to plastic zones *shorter* than expected. However, buckling was minimized in these experiments, as explained above. The last two factors also produce opposing effects which could affect the assumption of a constant traction at the elastic-plastic interface. (c) If the material exhibits a small amount of work hardening, the boundary traction would be a function of the amount of strain and the solution would yield *shorter* plastic bands. (d) On the other hand, if the load that results from the necking solution is assumed as the boundary traction, the solution would yield *longer* plastic zones. Either both factors are negligible in

the present experiments, or they combine in such a way that their individual effects cancel for values of T/Y below that required for initiation of slit growth. Their effects gain importance with increasing values of T/Y thus making the data points near failure less conclusive. However, the experimental slit growth initiation points substantiate the values predicted by the model as can be seen from Fig. 7.

CONCLUDING REMARKS

A model has been presented for predicting the initiation of growth of a slit in a sheet under tension, when plastic deformations are important and the slit has arbitrary orientation with respect to the tensile axis. The length of the confined plastic zones that grow from the tips of the slit has been related to the applied traction and the orientation of the slit. Relating the width of these plastic zones to the thickness of the sheet through a plastic necking solution resulted in a slit growth initiation criterion.

The slow propagation suggested by the present work differs substantially from that advanced by Goodier and Field [2]. To make the comparison simpler, only the slit normal to the tensile axis need be considered. Denoting the displacement at the end of the slit by $u_e(a)$, Goodier and Field obtained the following relationship to T/Y:

$$u_e(a) = C\,a \ln \sec \frac{\pi T}{2Y}, \tag{15}$$

where $C = (1/\pi)\,(\kappa + 1)\,(1 + \nu)\,(Y/E)$ is a constant, and suggested that slow extension of the slit under constant T and for constant Y (no strain hardening) took place at

$$\frac{u_e(a)}{a} = \text{constant}.$$

Their conclusion results from a dimensional argument. However, the deformations at the critical place where failure occurs are out of the plane of the sheet, and consequently, the problem does not lend itself to dimensional arguments. The propagation condition would become

$$\frac{u_e(a)}{t} = \text{constant},$$

which implies that, for a given sheet thickness, an *increase* in the slit length a may take place with a *decrease* of the applied traction T. This also implies that if T were to remain constant, an instability of the slit growth would result. This, as well as its experimental verification, awaits further investigation.

The bounds of applicability of the model presented in this report were only briefly and qualitatively explored. The effect of assuming different traction conditions at the elastic-plastic interface as well as the effect of buckling and finiteness of the specimen could be investigated in detail.

the present experiments, or they combine in such a way that their individual effects cancel for values of T/Y below that required for initiation of slit growth. Their effects gain importance with increasing values of T/Y thus making the data points near failure less conclusive. However, the experimental slit growth initiation points substantiate the values predicted by the model as can be seen from Fig. 7.

CONCLUDING REMARKS

A model has been presented for predicting the initiation of growth of a slit in a sheet under tension, when plastic deformations are important and the slit has arbitrary orientation with respect to the tensile axis. The length of the confined plastic zones that grow from the tips of the slit has been related to the applied traction and the orientation of the slit. Relating the width of these plastic zones to the thickness of the sheet through a plastic necking solution resulted in a slit growth initiation criterion.

The slow propagation suggested by the present work differs substantially from that advanced by Goodier and Field [2]. To make the comparison simpler, only the slit normal to the tensile axis need be considered. Denoting the displacement at the end of the slit by $u_e(a)$, Goodier and Field obtained the following relationship to T/Y:

$$u_e(a) = C\,a \ln \sec \frac{\pi T}{2Y}, \tag{15}$$

where $C = (1/\pi)\,(\kappa + 1)\,(1 + \nu)\,(Y/E)$ is a constant, and suggested that slow extension of the slit under constant T and for constant Y (no strain hardening) took place at

$$\frac{u_e(a)}{a} = \text{constant}.$$

Their conclusion results from a dimensional argument. However, the deformations at the critical place where failure occurs are out of the plane of the sheet, and consequently, the problem does not lend itself to dimensional arguments. The propagation condition would become

$$\frac{u_e(a)}{t} = \text{constant},$$

which implies that, for a given sheet thickness, an *increase* in the slit length a may take place with a *decrease* of the applied traction T. This also implies that if T were to remain constant, an instability of the slit growth would result. This, as well as its experimental verification, awaits further investigation.

The bounds of applicability of the model presented in this report were only briefly and qualitatively explored. The effect of assuming different traction conditions at the elastic-plastic interface as well as the effect of buckling and finiteness of the specimen could be investigated in detail.

REFERENCES

1. D.S. Dugdale, *J. Mech. Phys. Solids* 8, 100-104 (1960).
2. J.N. Goodier and F.A. Field, in *Fracture of Solids* (Wiley, 1963), pp. 103-118.
3. F.M. Burdekin and D.E.W. Stone, *J. Strain Analysis* 1, 145-153 (1966).
4. G.T. Hahn and A.R. Rosenfield, *Acta Metall.* 13, 293-306 (1965).
5. D.P. Isherwood and J.G. Williams, *Eng. Fract. Mech.* 2, 19-35 (1970).
6. E.H. Lee, *J. Appl. Mech.* 19, 331-336 (1952).
7. E.T. Onat and W. Prager, *J. Appl. Phys.* 25, 491-493 (1954).
8. D.P. Clausing, *Int. J. Fract. Mech.* 6, 71-85 (1970).
9. A.A. Griffith, *Proc. 1st Int. Congr. Appl. Mech.* (1924), pp. 55-63.
10. F.A. McClintock, *J. Basic Eng. Trans. ASME* 85D, 525-527 (1963).
11. F. Erdogan and G.C. Sih, *ibid.*, pp. 519-525.
12. M.L. Williams, *J. Appl. Mech.* 24, 109-114 (1957).
13. B. Cotterell, *Int. J. Fract. Mech.* 5, 251-252 (1969).
14. J.G. Williams and P.D. Ewing, *ibid.* 8, 441-446 (1972).
15. I. Finnie and A. Saith, *ibid.* 9, 484-486 (1973).
16. S.A. Marinshaw and G.H. Lindsey, *ibid.* 11, 273-282 (1975).
17. S.C. Sanday, *Plane Stress Elastic Strain Field and Plastic Enclaves Around a Slit*, Ph.D. Thesis (Carnegie Institute of Technology, 1967).
18. N.I. Muskhelishvili, *Some Basic Problems of the Mathematical Theory of Elasticity* (P. Noordhoff, Groningen, 1953).
19. S.C. Sanday, *SIAM J. Appl. Math.* 18, 815-817 (1970).
20. O. Richmond, *J. Mech. Phys. Solids* 17, 83 (1969).
21. ASTM, "Symposium on Fracture Toughness Testing and Its Applications," Special Technical Publication 381 (1965).
22. ASME, *A Review of Engineering Approaches to Design Against Fracture*, Subcommittee on Brittle Fracture, J.E. Strawley, Chairman (Am. Soc. Mech. Eng., New York).
23. D.C. Drucker, NYO-2394-27, Brown University, June 1967.

NOMENCLATURE

T	—	applied traction at infinity; T_{net}-nominal net section stress in experiments
$2a$	—	slit length
$\gamma\pi$	—	angle between slit and the normal to T
s	—	length of plastic zone
ℓ	—	$a + s$
u	—	width of plastic band at end of slit
$\Omega\pi$	—	angle between plastic band and slit directions
E	—	Young's modulus
ν	—	Poisson's ratio
Y	—	flow stress
t	—	sheet thickness
t_i	—	initial value of t
z, ζ	—	complex variables, $z = x + iy = re^{i\theta}$ $\zeta = \xi + i\eta = \rho e^{i\upsilon}$
ϵ_ℓ	—	longitudinal strain at the ends of the slit
ϵ_t	—	through-thickness strain at the ends of the slit
ω	—	mapping function
σ	—	value of ζ on unit circle
ϕ, ψ	—	stress functions
u_e	—	elastic displacement between two points on either side of the neck at the tip of the slit
u_{ec}	—	critical value for u_e
L	—	recorded load in experiments
R	—	slit-tip root radius = $d/2$
d	—	slit width
w	—	specimen width